Nutrition, Metabolism & Cardiovascular Diseases (2019) **29**, 409–420

Available online at www.sciencedirect.com

Nutrition, Metabolism & Cardiovascular Diseases

journal homepage: www.elsevier.com/locate/nmcd

Betulinic acid inhibits high-fat diet-induced obesity and improves energy balance by activating AMPK

K.-D. Kim [a,1], H.-Y. Jung [b,d,1], H.G. Ryu [c,1], B. Kim [a,d,1], J. Jeon [b,d], H.Y. Yoo [b], C.H. Park [f], B.-H. Choi [e], C.-K. Hyun [a], K.-T. Kim [b,c], S. Fang [g], S.H. Yang [h,i], J.-B. Kim [a,f,*]

[a] School of Life Science, Handong Global University, Pohang, Gyungbuk, South Korea
[b] Division of Integrative Biosciences and Biotechnology, POSTECH, Pohang, Gyungbuk, South Korea
[c] Department of Life Sciences, POSTECH, Pohang, Gyungbuk, South Korea
[d] R&D Center, NovMetaPharma Co., Ltd., Pohang, Gyungbuk, South Korea
[e] Advanced Bio Convergence Center, Pohang Technopark, Pohang, Gyungbuk, South Korea
[f] Mistle Biotech Co., Ltd., Pohang, Gyungbuk, South Korea
[g] Severance Biomedical Science Institute, BK21 PLUS Project for Medical Science, Yonsei University College of Medicine, Seoul, South Korea
[h] Kidney Research Institute, Seoul National University College of Medicine, Seoul, South Korea
[i] Seoul National University Biomedical Research Institute, Seoul, South Korea

Received 29 August 2018; received in revised form 5 December 2018; accepted 5 December 2018
Handling Editor: Gian Luigi Russo
Available online 8 January 2019

KEYWORDS
Betulinic acid;
Anti-obesity;
Energy balance;
Non-alcoholic fatty liver disease;
Metabolic syndromes;
AMPK

Abstract *Background and aim:* Metabolic syndromes are prevalent worldwide and result in various complications including obesity, cardiovascular disease and type II diabetes. Betulinic acid (BA) is a naturally occurring triterpenoid that has anti-inflammatory properties. We hypothesized that treatment with BA may result in decreased body weight gain, adiposity and hepatic steatosis in a diet-induced mouse model of obesity.
Methods and results: Mice fed a high-fat diet and treated with BA showed less weight gain and tissue adiposity without any change in calorie intake. Gene expression profiling of mouse tissues and cell lines revealed that BA treatment increased expression of lipid oxidative genes and decreased that of lipogenesis-related genes. This modulation was mediated by increased AMP-activated protein kinase (AMPK) phosphorylation, which facilitates energy expenditure, lipid oxidation and thermogenic capacity and exerts protective effects against obesity and nonalcoholic fatty liver disease. Overall, BA markedly inhibited the development of obesity and nonalcoholic fatty liver disease in mice fed a high-fat diet, and AMPK activation in various tissues and enhanced thermogenesis are two possible mechanisms underlying the antiobesity and antisteatogenic effects of BA.
Conclusions: The current findings suggest that treatment with BA is a potential dietary strategy for preventing obesity and nonalcoholic fatty liver disease.

Introduction

Metabolic syndrome is a state of metabolic dysregulation characterized by abdominal obesity, insulin resistance, dyslipidemia, hypertension, fatty liver disease and other disorders [1]. The prevalence of metabolic syndrome is increasing rapidly in developing countries as well as in advanced countries. Because many risk factors are

* Corresponding author. School of Life Science, Handong Global University, Pohang, Gyungbuk 37554, South Korea. Fax: +82 54 261 6705.
E-mail address: i1948@naver.com (J.-B. Kim).
[1] These authors contributed equally to this work.

https://doi.org/10.1016/j.numecd.2018.12.001
0939-4753/

associated with metabolic syndrome, no drug can effectively inhibit all risk factors in the long term. Therefore, interest in therapeutic strategies that might target multiple risk factors is increasing [2].

Excess fat accumulation might be related to insulin resistance and the inability to appropriately store energy and ultimately determines susceptibility to metabolic syndrome development [3]. The major cause of obesity is defective cellular metabolism [4], suggesting impaired mitochondrial fatty acid oxidation [5]. Subtle variations in thermogenesis related to uncoupling proteins might also be important for maintaining body weight and energy balance [6]. Therefore, focusing on obesity, insulin resistance and energy metabolism is important when studying metabolic syndrome.

In rodents and small mammals, brown adipose tissue (BAT)-mediated thermogenesis is key for maintaining core body temperature at temperatures below thermoneutrality [7]. Substantial evidence also indicates that BAT thermogenesis plays a crucial role in regulating energy balance by utilizing excess calories [8–12]. BAT dysfunction induced by UCP1 deficiency increases susceptibility to diet-induced obesity [12–14]. In contrast, enhancement of thermogenic activity through uncoupling protein 1 (UCP-1) overexpression or by BAT activators such as cold exposure, β-adrenergic receptor agonists, bile acids, and fibroblast growth factor 21 reduces dietary and genetic obesity [15–18].

AMP-activated protein kinase (AMPK) is a "cellular fuel gauge" that acts to simultaneously shut down ATP-consuming biosynthetic processes and facilitate ATP-producing catabolic processes during periods of metabolic stress, leading to rapid changes in fatty acid metabolism, and AMPK phosphorylation stimulates fatty acid metabolism [19]. In many tissues, including skeletal muscle, glucose transporter type 4 (GLUT4) translocation to the plasma membrane occurs in response to stimuli such as muscle contraction and insulin, and increased GLUT4 expression may be controlled by AMPK phosphorylation of peroxisome proliferator-activated receptor gamma coactivator-1 alpha (PGC-1α) as well as other transcription factors [20]. PGC-1α, which was identified based on its interaction with PPARγ in brown fat and skeletal muscle in response to cold exposure [21], is known to be involved in regulating energy metabolism, thermogenesis and other biological processes that control the phenotypic characteristics of various organs [22–24].

Betulinic acid (BA), widely distributed in the outer bark of a variety of tree species [25], is a naturally occurring pentacyclic triterpenoid [26]. Clinical use of BA is hindered by its low water solubility, which greatly limits its bioavailability and therapeutic applications [27]. To overcome this solubility problem, cyclodextrin complexation has been accomplished using β- and γ-derivatives that have high water solubility [28], and due to the bulky structure of BA, the latter were found to be the most appropriate (Supplementary Fig. 1A). BA exhibits a wide variety of pharmacological and biochemical effects, including the following: anti-inflammatory, anti-cancer [29–31], anti-bacterial [32], anti-malarial [33], anti-angiogenesis [34], and antiviral [35] activities; induction of cell death via the MAPK pathway [36]; and immunomodulatory effects via production of proinflammatory cytokines and recruitment of macrophages [37]. Most studies involving BA have focused on its anti-cancer effects, yet there is increasing interest in the hypoglycemic [38] and hypolipidemic activities and their potential to reduce abdominal fat, glucose tolerance [39] and nonalcoholic fatty liver disease [40]. Although BA has been suggested to prevent abdominal fat accumulation and the development of fatty liver in mice, few reports have examined the beneficial effects of BA in various tissues of obese animals. The aim of this study was to investigate whether BA attenuates high-fat diet (HFD)-induced obesity and fatty liver in mice. Furthermore, to reveal the underlying mechanism of action at the molecular level, we examined the effect of BA on expression of genes and proteins involved in energy metabolism, fatty acid oxidation and inflammation. Our data reveal that BA reduced lipid accumulation in 3T3-L1 adipocytes and decreased adiposity changes, serum lipids and adipokines in HFD-fed mice. BA also protected mice against HFD-induced hepatic steatosis and decreased expression of inflammatory genes and lipogenic genes. BA enhanced thermogenesis during hypothermia, gene expression related to energy expenditure and fatty acid oxidation in BAT and skeletal muscle. Taken together, our results support the use of potential therapeutic agents for preventing or treating obesity and fatty liver through enhanced fatty acid oxidation, energy metabolism and anti-inflammatory effects.

Methods

Materials

BA (purity, > 97%) was purchased from TCI (Tokyo, Japan), and dorsomorphin (Compound C) was obtained from Sigma–Aldrich (St. Louis, Missouri, USA). Dulbecco's modified Eagle's medium (DMEM), bovine calf serum (BCS), fetal bovine serum (FBS) and penicillin/streptomycin were purchased from HyClone Laboratories (Logan, UT). Antibodies against phospho-AMPKα (Thr172), total-AMPK, phospho-ACC (Ser79) and total-ACC were obtained from Cell Signaling Technology (Beverly, MA), against PGC-1α and β-actin were purchased from Santa Cruz Biotechnology Inc. (Dallas, TX), and against UCP-1 was purchased from Abcam (Cambridge, UK). West Femto Chemiluminescent substrate was purchased from PIERCE (Rockford, IL). Horseradish peroxidase-conjugated anti-rabbit secondary antibodies were obtained from Santa Cruz Biotechnology Inc. Nitrocellulose membranes and X-ray films were purchased from Whatman (Dassel, Germany) and AGFA (Mortsel, Belgium), respectively. SYBR Green master mix for real-time quantitative PCR was purchased from the USB Corporation (Cleveland, OH).

Cell culture and treatment

3T3-L1 mouse embryo fibroblasts and the hibernoma-derived mouse brown adipocyte cell line HIB1B were grown in high-glucose DMEM containing 10% BCS at 37 °C in a 5% CO_2 incubator. To differentiate both types of pre-adipocytes into adipocytes, postconfluent (3 days) cells were incubated in DMEM containing 10% FBS supplemented with 0.5 mM isobutylmethyl xanthine, 1 μM dexamethasone, and 1 μg/mL insulin (day 0). At day 2, the medium was carefully replaced with DMEM containing 10% FBS supplemented with 1 μg/mL insulin. After 2 days, the medium was replaced with DMEM containing 10% FBS every 2 days for the next 4 days. AML12 mouse hepatocyte cells were cultured in 5% CO_2 at 37 °C in DMEM/F12 medium (GibcoBRL, Grand Island, NY) containing L-glutamine, 2.438 g/L sodium bicarbonate, 40 ng/mL dexamethasone, 10% FBS and a mixture of insulin, transferrin, and selenium (ITS; Sigma, St. Louis, MO). To induce hepatic steatosis *in vitro*, cells were treated with palmitic acid (Sigma–Aldrich, St. Louis, MO), which was dissolved at 60 °C in 50 mM KOH to obtain a 30 mM stock solution; a 10% (w/v) solution of fatty-acid-free BSA was prepared in serum-free DMEM/F12. The two solutions were combined to produce BSA-conjugated palmitate. The mixture was further diluted in DMEM/F12 to reach the desired final concentrations. Cells were treated with the 250 μM palmitic acid/BSA mixture for 1 day to induce hepatic steatosis. C2C12 cells were maintained in DMEM containing 10% FBS until the cells were approximately 80% confluent. To induce myotube differentiation, the C2C12 growth medium was replaced with DMEM containing 2% horse serum at day 0, and C2C12 myotubes were treated with BA on day 7. Cells were treated with BA or 0.5% DMSO for 20 h, and independently, cells were pretreated with 40 μM AMPK inhibitor (compound C) for 2 h and then exposed to BA for an additional 20 h.

Animals and diets

Lean male C57BL/6 mice (6 weeks old) were purchased from Central Lab Animal Inc. (Seoul, Korea). All animal experiments were approved by the Ethics Review Committee of Handong Global University, Republic of Korea, and conducted in accordance with approved guidelines. Twenty healthy mice were assigned to one of four groups. Mice were maintained in a specific pathogen-free animal facility under a standard 12-hour light/12-hour dark cycle. To examine diet-induced obesity, mice were fed with either normal rodent chow or a HFD (Central Lab Animal Inc.) for 11 weeks. The standard chow diet contained 28.5% protein, 13.5% fat, and 58.0% carbohydrate, and the HFD contained 18.4% protein (casein), 60.3% fat, and 21.3% carbohydrate. In addition, 150 mg/kg BA or 10% ethanol PBS, as the vehicle control, was orally administered daily for 11 weeks. At the conclusion of the *in vivo* experiment, mice were sacrificed, and adipose, liver, and quadriceps tissues were removed and fixed in 10% paraffin for histology. The remaining tissues were snap-frozen in aluminum tongs cooled to the temperature of liquid nitrogen. Samples were stored at −80 °C until analysis.

Cold exposure test

After 11 weeks of BA treatment, mice were fasted overnight, and their core body temperature was measured with a clinical rectal thermometer (Thermalert model TH-5; Physitemp Instruments LLC., Clifton, NJ) every 30 min in a 4 °C cold room until the mice exhibited hypothermia.

Analysis of blood biochemical parameters

The mice were fasted for 12 h before sacrifice using CO_2 gas, and whole blood samples were obtained by cardiac puncture. Serum was prepared by centrifugation at 2000×*g* at 24 °C for 30 min and then stored at −80 °C. Serum total cholesterol and triglyceride levels were detected using an INFINITY kit (Thermo Fisher Scientific Inc., Middletown, USA). Insulin levels were determined with a Mouse Ultrasensitive Insulin ELISA kit (ALPCO Diagnostics, Windham, NH), and leptin levels were measured with a Mouse Leptin ELISA kit (Morinaga Institute of Biological Science, Inc., Yokohama, Japan).

Histology

Hematoxylin-eosin (H&E) staining was performed according to the protocols of Jung et al. [41], with slight modifications. Briefly, tissues were fixed in 10% formalin, processed and embedded in paraffin prior to sectioning. Ten-micrometer thick sections were affixed to slides, deparaffinized, dehydrated, and then stained with H&E. Stained liver and adipose tissue sections were observed under a light microscope (BX 50, Olympus, Tokyo, JAPAN) at 400X magnification.

Western blotting analysis

Cells were harvested, and tissues were homogenized with PRO-PREP protein extraction solution purchased from iNtRON Biotechnology (Seongnam, Korea) with 10 mM NaF, 2 mM Na_3VO_4 (pH 7.4), and 10 mM $Na_4P_2O_7$ and incubated for 1 h at 4 °C. The solution was centrifuged at 13,000 rpm at 4 °C for 10 min to remove insoluble materials and lipids. The protein concentration in the tissues was measured using the Bradford reagent (Bio-Rad, Hercules, CA) with bovine serum albumin as a standard. Equal quantities of proteins were separated by SDS-PAGE and then transferred to a nitrocellulose membrane (Bio-Rad). The membrane was blocked with 10% skim milk for 2 h at room temperature and then incubated overnight at 4 °C with primary antibodies. The membranes were washed with TBS-T 3 times and then incubated for 1 h at room temperature with a horseradish peroxidase-conjugated secondary antibody. After washing the membrane with TBS-T 3 times, the signals

were detected with SuperSignal West Femto Chemiluminescent substrate.

Oil red O staining

3T3-L1 cells were washed with cold PBS three times, fixed in 10% formalin for more than 1 h at 4 °C, and then stained for 1 h at room temperature in freshly diluted oil red O solution. The stained cells were treated with 100% isopropyl alcohol to extract oil red O, and the colorimetric intensity of the extract was measured at 500 nm to determine the lipid content.

Real-time quantitative PCR

Total RNA from each tissue was extracted using an Easyspin TM Total RNA extraction kit (iNtRON Biotechnology) according to the manufacturer's instructions. cDNA was synthesized from 1 μg of DNase-treated total RNA using M-MLV reverse transcriptase (Invitrogen). PCRs were conducted with SYBR Green master mix, and the results are expressed after normalization to the 36B4 mRNA level in the same sample. Analysis was performed using an ABI 7500 Fast Real Time PCR system (Applied Biosystems). Amplification of real-time PCR was performed according to the protocols of Jung et al. [42], with slight modifications. Briefly, the reaction was performed at 94 °C for 10 min, followed by 40 cycles of amplification (95 °C for 15 s, 60 °C for 1 min). A melting curve was produced to confirm a single gene-specific peak and detect primer/dimer formation by heating the samples from 65 to 95 °C in 0.5 °C increments with a dwell time of 10 s at each temperature while continuously monitoring fluorescence. Quantification of gene transcripts was performed with gene-specific primers (Table 1).

Table 1 Real-time quantitative PCR primer sequences.

Gene	Orientation	Primer sequence (5′ → 3′)
Arbp	Forward	TCACTGTGCCAGCTCAGAAC
	Reverse	AATTTCAATGGTGCCTCTGG
PGC-1α	Forward	TCGATGTGTCGCCTTCTTGC
	Reverse	ACGAGAGCGCATCCTTTGG
UCP1	Forward	GGCCCTTGTAAACAACAAAATAC
	Reverse	GGCAACAAGAGCTGACAGTAAAT
UCP2	Forward	ACCAAGGGCTCAGAGCATGCA
	Reverse	TGGCTTTCAGGAGAGTATCTTTG
UCP3	Forward	CCAACATCACAAGAAATGC
	Reverse	TACAAACATCATCACGTTCC
Cpt-1α	Forward	ACTCTTGGAAGAAGTTCA
	Reverse	AGTATCTTTGACAGCTGGGAC
Cpt-2	Forward	CTGTCAGCCTTACACTGACCC
	Reverse	AGGAAGGGAGGATGAGACGT
Acox1	Forward	ACA CTA ACA TAT CAA CAA GAG GAG
	Reverse	CAT TGC CAG GAA GAC CAG
L-FABP	Forward	CACACAGCTGAGATCATGGC
	Reverse	AGCAGGAGGTGCAAGTATGG
MCAD	Forward	GATCGCAATGGGTGCTTTTGATAGAA
	Reverse	AGCTGATTGGCAATGTCTCCAGCAAA
SREBP1c	Forward	GGAGCCATGGATTGCACATT
	Reverse	GGCCCGGGAAGTCACTGT
F4/80	Forward	CCCAGCTTATGCCACCTGCA
	Reverse	TCCAGGCCCTGGAACATTGG
IL-1α	Forward	CAAACTGATGAAGCTCGTCA
	Reverse	TCTCCTTGAGCGCTCACGAA
IL-1β	Forward	TCTGGGGTTGATGTAGGA
	Reverse	GGGCTGGAAAAATGGTC
IL-6	Forward	GACAACTTTGGCATTGTGG
	Reverse	ATGCAGGGATGATGTTCTG
TNF-α	Forward	CATCTTCTCAAAATTCGAGTGACAA
	Reverse	TGGGAGTAGACAAGGTACAACCC
ApoC2	Forward	GCAGGGCTCCCTCTTAAGTT
	Reverse	AAAATGCCTGCGTAAGTGCT
RBP4	Forward	AGGAGAACTTCGACAAGGCT
	Reverse	TTCCCAGTTGCTCAGAAGAC
LPL	Forward	ACTCGCTCTCAGATGCCCTA
	Reverse	TTGTGTTGCTTGCCATTCTC
FAS	Forward	GCTGCGGAAACTTCAGGAAAT
	Reverse	AGAGACGTGTCACTCCTGGACTT
SCD1	Forward	CCTGCCTCTTCGGGATTT
	Reverse	TTGTGAGGGTCGGCGTGT
GLUT2	Forward	ATCTGGCTCCGCACTCTCATTCTTG
	Reverse	CCCTGTGACTTTTCTGTGTTCTTAGG
GLUT4	Forward	AACCAGCATCTTCGAGTCGG
	Reverse	CGAGACCAACGTGAAGACCG
DGAT1	Forward	TCAGATTGAGAAGCGCCTGG
	Reverse	ACGGAACCCACTGGAGTGAT
DGAT2	Forward	GCCGATGGGTCCAGAAGAAGTT
	Reverse	CTCCAGCTTGGGGACAGTGATG
GPAT	Forward	CAGACACAGGCAGGGAATCC
	Reverse	GCCTAGGTCGAAATCGCGAG
PPARγ	Forward	AGTGGAGACCGCCCAGG
	Reverse	GCAGCAGGTTGTCTTGGATGT

Statistical analysis

Statistical analyses were performed using GraphPad Prism software (version 5.0 GraphPad Software, La Jolla, CA). The data were analyzed with Student's t-test or one-way analysis of variance (ANOVA) followed by Tukey's post hoc test, and the results are presented as the means ± S.D. All p values < 0.05 were considered statistically significant.

Results

BA decreases adiposity changes, serum lipids and adipokines in HFD-fed mice

During the 11-week experiment, body weight and food intake were measured weekly. As shown in Fig. 1A, the BA-treated group showed a slight decrease in body weight compared to the control group. However, this effect was significantly pronounced in animals that were fed a HFD with BA. The difference between the BA-treated and control animals became significant at week 7. At the end of the experiments, the body weight of mice treated with BA was 10% lower ($p < 0.05$) than that of the control group in the HFD group, with no difference in food intake (Fig. 1B). To test whether body weight loss was caused by decreased adiposity, animals were sacrificed, and white adipose tissue (WAT) and BAT were dissected and weighed. The weights of WAT, including inguinal,

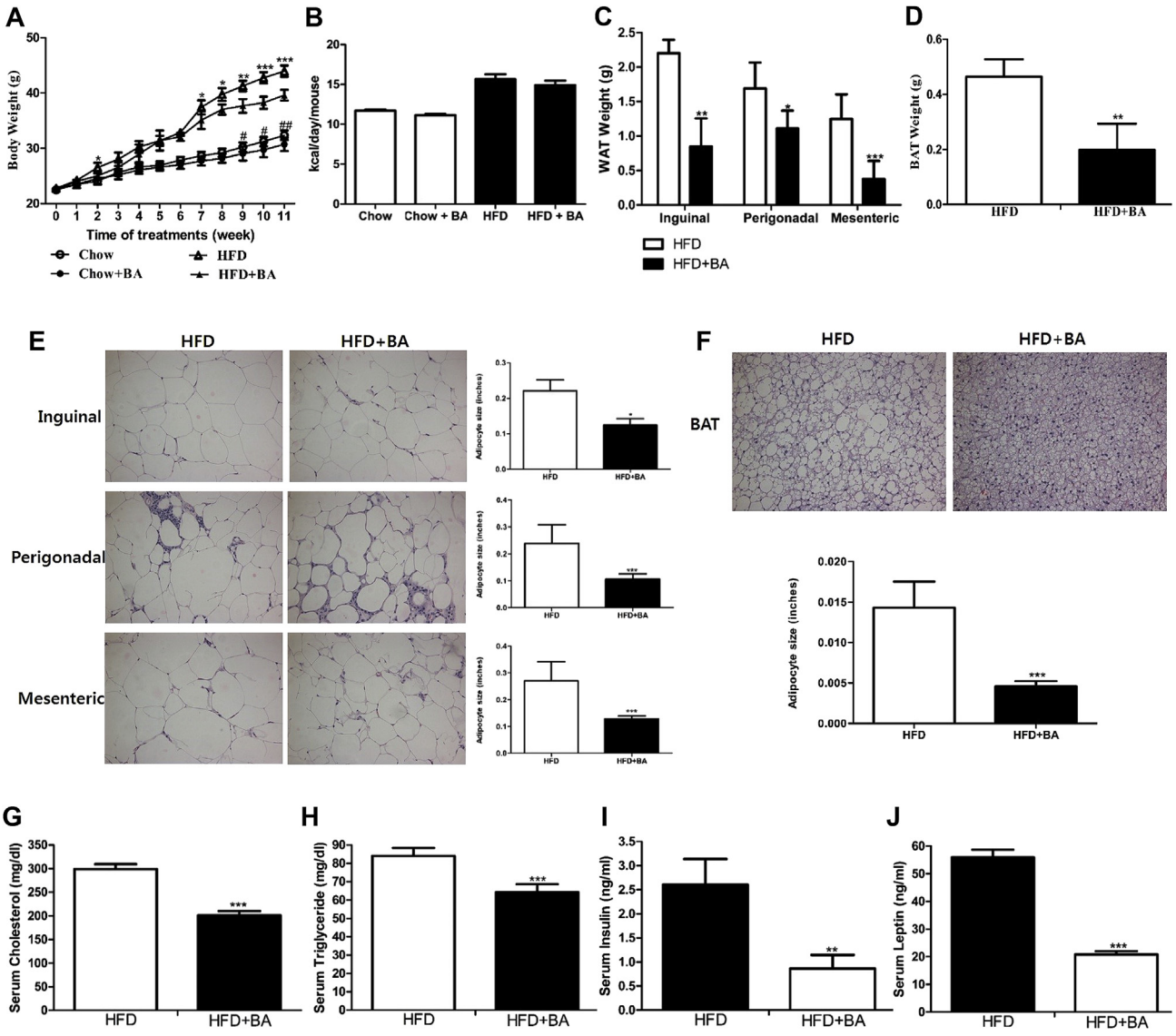

Figure 1 BA decreases adiposity changes and serum lipid and adipokine levels in HFD-fed mice and reduces lipid accumulation in 3T3-L1 adipocytes. BA was orally administered at 150 mg/kg for 11 weeks. A, Body weights of wild-type (WT) or BA-treated (BA) mice during exposure to a chow diet or HFD. B, Average food intake expressed as kcal/mouse/day. C and D, Fat mass of WAT and BAT in WT and BA mice after 11 weeks of exposure to HFD. E and F, Representative H&E-stained sections of WAT and BAT from WT and BA mice are shown. Adipocyte sizes were measured with ImageJ analysis software (right). G-J, Fasting serum cholesterol, triglyceride, insulin and leptin levels in nontreated and BA-treated mice are shown. n = 5 per group; means ± S.D.; $^{*}p < 0.05$, $^{**}p < 0.005$, $^{***}p < 0.0005$ versus the HFD group; $\#p < 0.05$, $\#\#p < 0.005$ versus the chow group.

perigonadal, mesenteric and BAT, were significantly decreased (inguinal; 62%, perigonadal; 35%, mesenteric; 70%, brown; 43%) in BA-treated mice (Fig. 1C, D). As expected, white and brown adipocytes were smaller in BA-treated mice than in control mice (Fig. 1E, F).

Because obesity is associated with elevated serum lipids, insulin and leptin, we used an enzymatic assay reagent or kit to measure these components. BA-treated mice displayed a 34% decrease in cholesterol (Fig. 1G), a 24% decrease in serum triglyceride (Fig. 1H), a 2.7-fold reduction in fasting insulin (Fig. 1I), and a 2.9-fold decrease in leptin (Fig. 1J). These results suggest that BA alleviates the metabolic phenotypes of obese mice.

BA reduces lipid accumulation and increases expression of genes associated with energy metabolism in 3T3-L1 adipocytes by activating AMPK

When fully differentiated 3T3-L1 adipocytes were treated with BA for 20 h and stained with oil red O, lipid accumulation was significantly reduced in a dose-dependent manner (Fig. 2A). To investigate the antiadipogenic mechanism, the effect of BA on the expression levels of mRNAs associated with energy expenditure and fatty acid oxidation was assessed. We used real-time RT-PCR to examine the mRNA levels of genes regulating energy expenditure, including PGC-1α, UCP-2, and of fatty acid

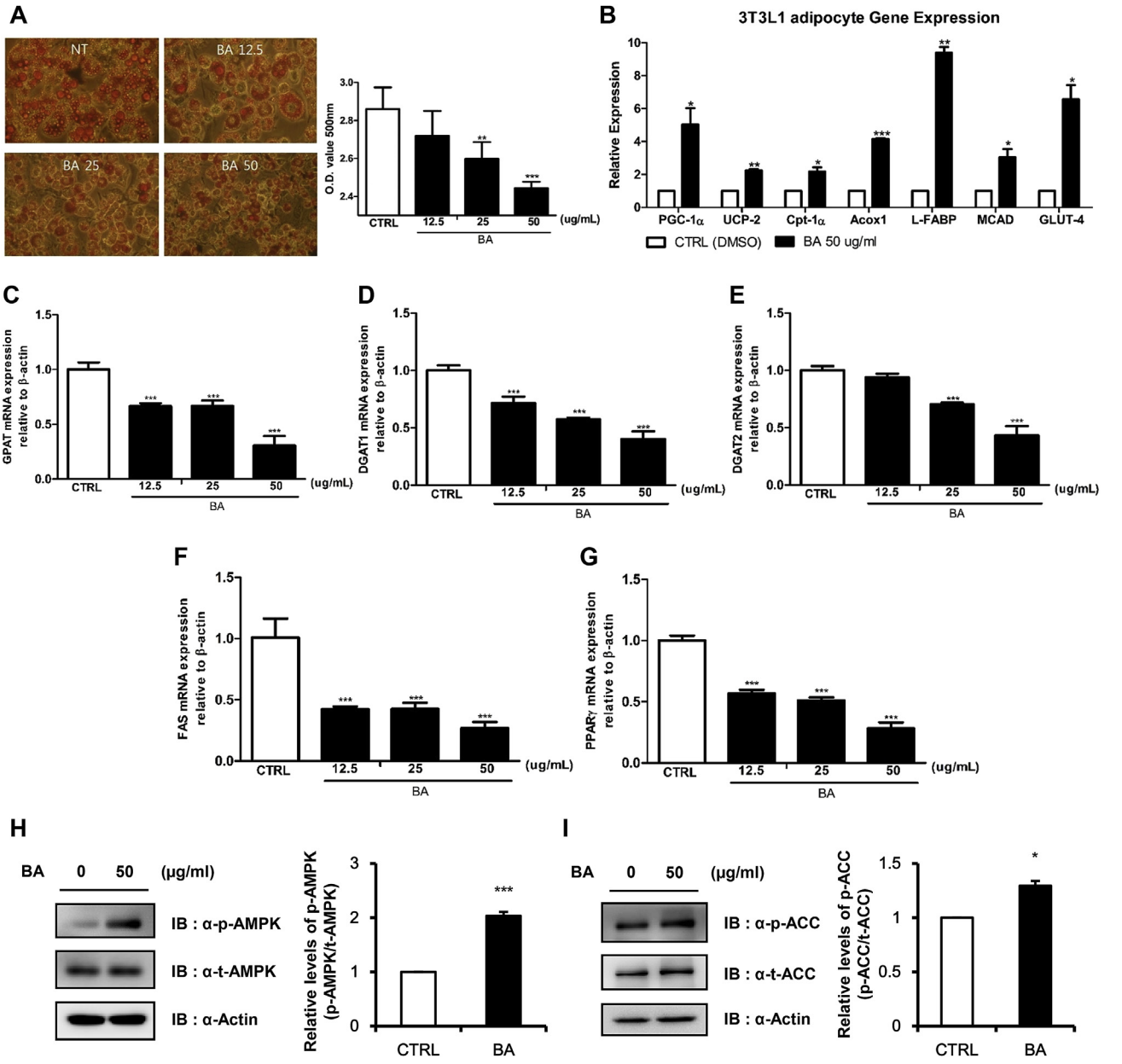

Figure 2 BA reduces lipid accumulation and increases expression of genes associated with energy metabolism in 3T3-L1 adipocytes by activating AMPK. Cells were treated with BA in serum-free DMEM in a dose-dependent manner (12.5, 25, 50 μg/mL of BA or DMSO) for 20 h and then washed in ice-cold PBS. Cells were fixed in 10% formalin. Pictures were taken after the cells were stained for 1 h at room temperature with freshly diluted oil red O solution. A, Stained cells were treated with 100% isopropyl alcohol to extract oil red O (left), and the lipid content was determined by colorimetric measurement of the oil red O stain extract at 500 nm (right). B, Relative mRNA expression levels of genes related to energy metabolism and fatty acid oxidation in 3T3-L1 adipocytes. C-G, mRNA levels of lipid anabolism-related genes including Gpat, Dgat1, Dgat2, FAS and PPAR-γ in differentiated 3T3-L1 cells were analyzed using real-time PCR. H and I, AMPK and ACC activation was detected by Western blotting analysis in differentiated 3T3-L1 cells. n = 3–7 per group; means ± S.D.; $^{*}p < 0.05$, $^{**}p < 0.005$, $^{***}p < 0.0005$ compared to CTRL. (For interpretation of the references to colour in this figure legend, the reader is referred to the Web version of this article.)

oxidative genes, including carnitine palmitoyltransferase (Cpt)-1, acyl-coenzyme A oxidase 1 (Acox1), L-fatty acid binding protein (FABP) and medium-chain acyl-coenzyme A dehydrogenase (MCAD). Consistent with the *in vivo* and *in vitro* results, mRNA levels were higher in BA-treated 3T3-L1 adipocytes than in nontreated cells (Fig. 2B). Additionally, BA-treated 3T3-L1 adipocytes cells showed reductions in expression of transcription factors required for adipocyte differentiation (PPARγ) and enzymes involved in triglyceride synthesis (GPAT, DGAT1, DGAT2) and fatty acid synthase (FAS) (Fig. 2C–G). To evaluate whether AMPK, a key enzyme in energy homeostasis, is activated by BA during 3T3-L1 differentiation, the level of phosphorylated AMPKα was analyzed and compared with the total level of AMPKα by Western blotting. Levels of phosphorylated AMPKα and its target protein ACC were increased in the group treated with 50 μg/mL BA compared with those in the control group (Fig. 2H, I).

BA increases thermogenesis in hypothermia and gene expression related to energy expenditure and fatty acid oxidation in BAT

We next performed a cold test to assess the effect of BA on adaptive thermogenesis capacity. BA-treated animals maintained higher body temperatures than nontreated animals (Fig. 3A), suggesting that BA treatment improved thermogenic capacity. To test whether thermogenesis was accompanied by changes in the expression of genes involved in energy expenditure and fatty acid oxidation, total RNA was prepared from BAT. We examined the mRNA levels of genes regulating energy expenditure, including PGC-1α, UCP-1, UCP-2, and UCP-3, and fatty acid oxidative genes including Cpt-1α, Cpt-2, FABP and MCAD by real-time RT-PCR. Consistent with the *in vivo* results, mRNA levels in the BAT of BA-treated mice were elevated compared with those of nontreated mice (Fig. 3B), and protein expression levels of UCP-1 and PGC-1α (Fig. 3C, D) were higher in BA-treated HIB1B brown adipocytes. As AMPK is the main activator of fatty acid oxidation and thermogenesis, we evaluated whether BA can enhance AMPK activity and found that phosphorylated AMPK was increased in BA-

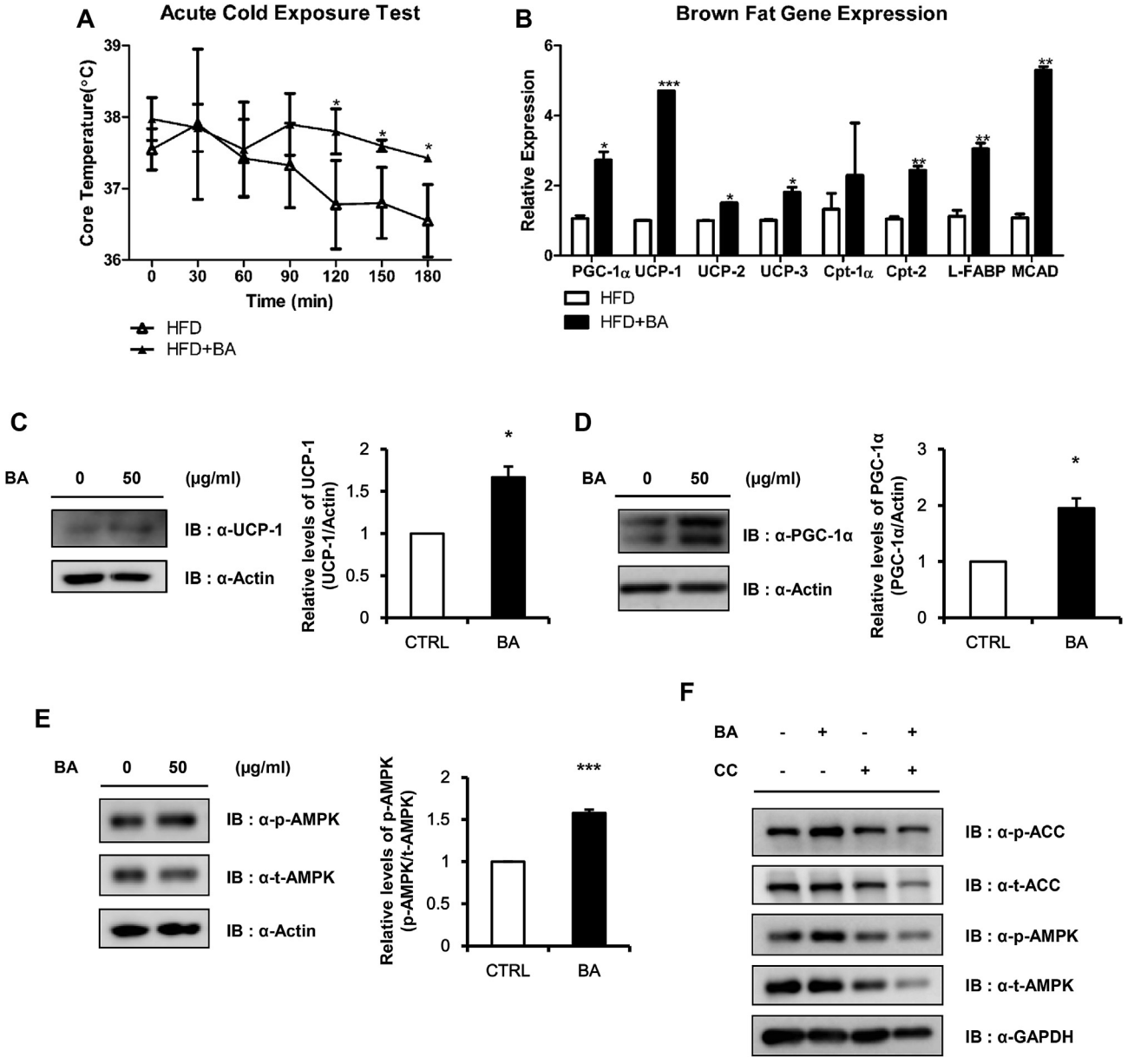

Figure 3 BA-treated mice show increased thermogenesis and expression of genes associated with energy expenditure and fatty acid oxidation. A, Rectal temperatures of WT and BA mice placed at 4 °C are shown. B, The relative level of mRNA expression of genes related to energy expenditure and fatty acid oxidation in BAT is shown; means ± S.D.; $^{*}p < 0.05$, $^{**}p < 0.01$. C and D, Protein expression of UCP-1 and PGC-1α in BA-treated HIB1B cells. E, Change in the AMPK phosphorylation level due to BA treatment of HIB1B cells. F, Activation of AMPK and ACC was measured in HIB1B cells pretreated with an AMPK inhibitor followed by BA treatment for an additional 20 h; n = 3–5 per group; means ± S.D.; $^{*}p < 0.05$.

treated cells compared to nontreated cells (Fig. 3E), an increase that was reversed by AMPK inhibitor treatment (Fig. 3F).

BA improves energy metabolism in skeletal muscle

To investigate whether BA improves energy metabolism in skeletal muscle, we measured relative mRNA expression levels in the quadriceps of nontreated and BA-treated mice. Real-time quantitative PCR data showed that expression levels of fatty acid oxidative genes including PGC-1α, UCP-2, UCP-3, Cpt-1α, Cpt-2, L-FABP and the glucose transporter GLUT4 were increased in the quadriceps of BA-treated mice compared to those of nontreated mice (Fig. 4A). This BA-induced upregulation of lipid oxidative gene expression was confirmed by increased protein levels of PGC-1α and UCP-3 in C2C12 myotubes (Fig. 4B. C). We also measured the phosphorylation levels of AMPK in BA-treated mice and BA-treated cells and found that phosphorylated AMPK was increased in BA-treated mice or cells compared to that in nontreated mice or cells (Fig. 4D, E).

BA protects against HFD-induced hepatic steatosis

Because hepatic steatosis or fatty liver is highly associated with diet-induced obesity in humans and animal models, we next examined whether treatment with BA improved hepatic steatosis and fatty liver in HFD-fed mice. Small lipid vesicles were observed in the hepatocytes of BA-

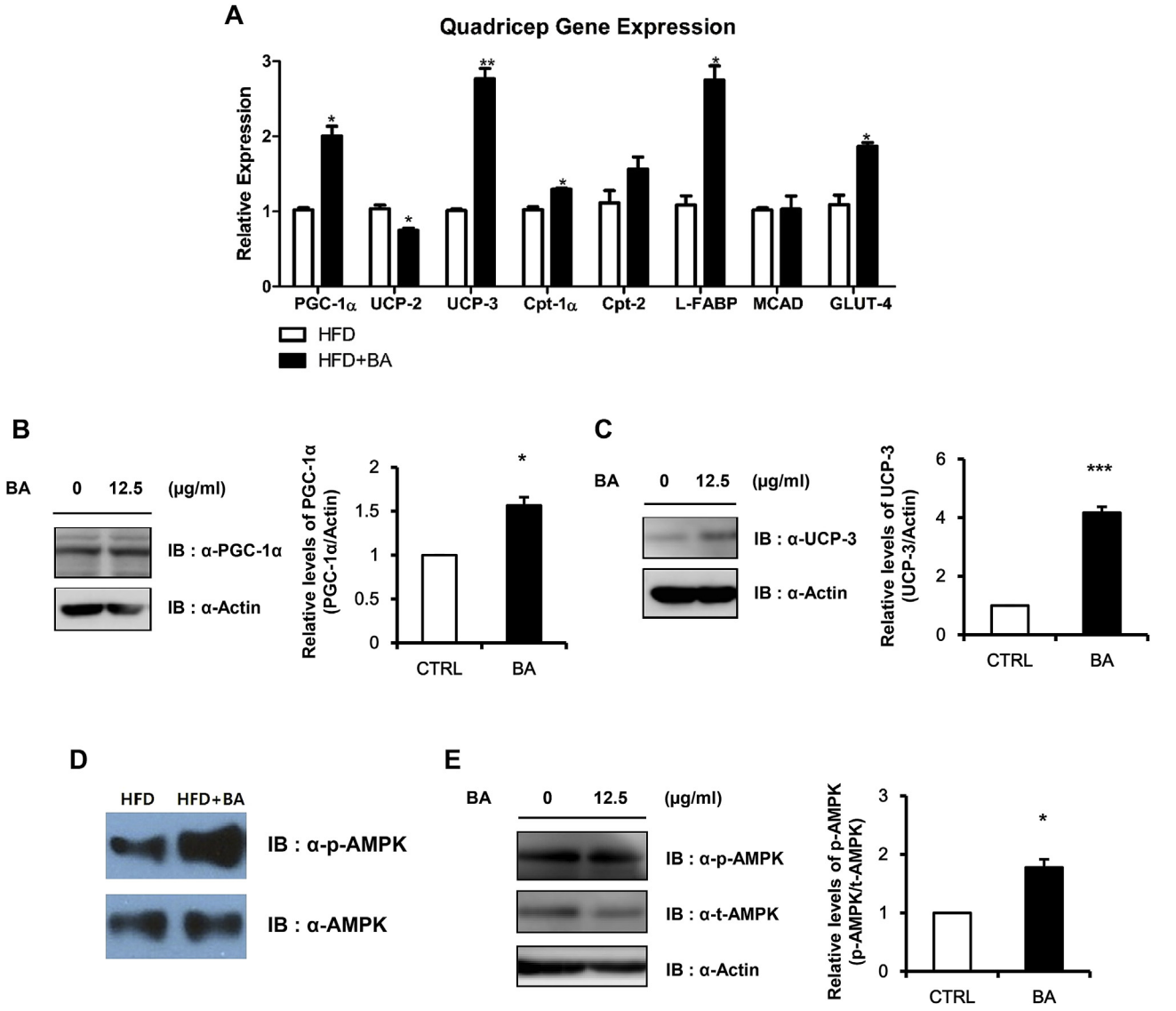

Figure 4 BA increases energy-related gene expression and activates AMPK. A, The relative amount of mRNA expression of genes related to energy expenditure, fatty acid oxidation and glucose transport in quadriceps tissue is shown. B and C, Protein expression levels of lipid oxidative genes, PGC-1α and UCP3 in C2C12 myotubes. D and E, Western blotting analysis was performed to detect the phosphorylation levels of AMPK in quadriceps tissue from nontreated and BA-treated mice or C2C12 myotubes. n = 3–5 per group; means ± S.D.; $^{*}p < 0.05$, $^{**}p < 0.01$, $^{***}p < 0.001$.

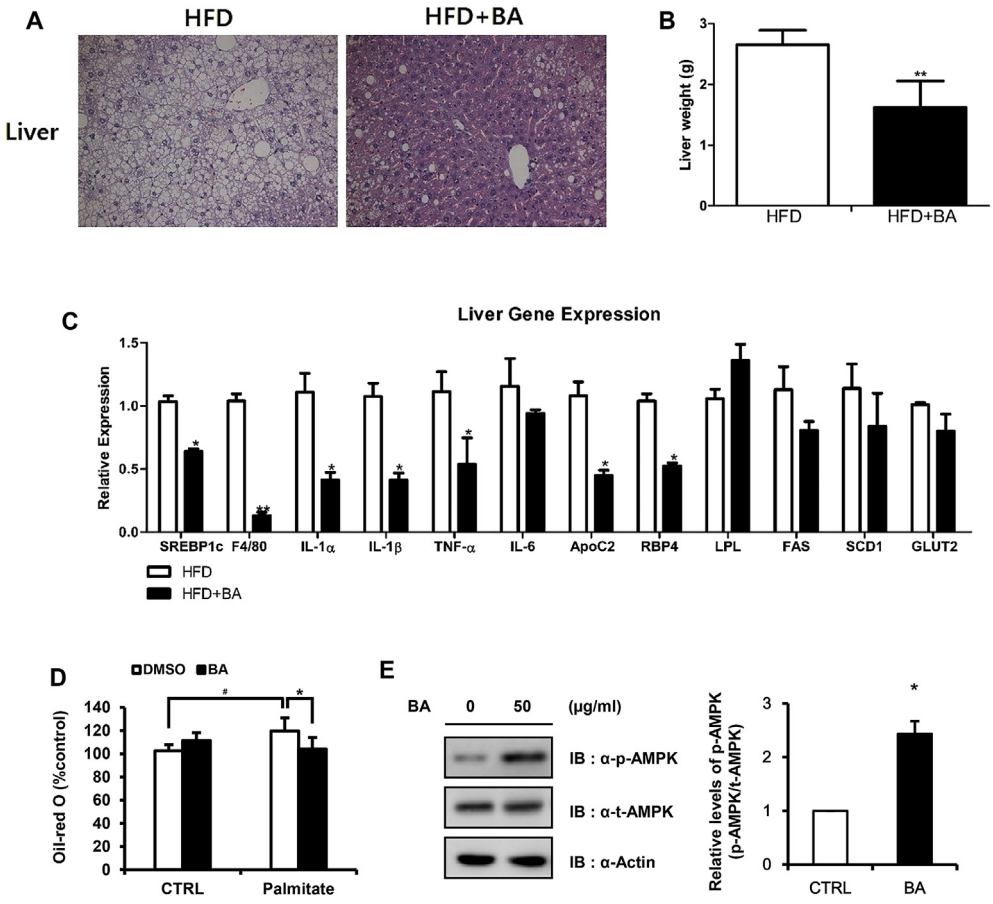

Figure 5 BA inhibits hepatic steatosis and reduces expression of genes associated with inflammation and lipid synthesis by activating AMPK. A, H&E staining of histological sections from the livers of WT and BA mice is shown. B, Liver weights were decreased in BA mice. C, The relative amount of mRNA expression of genes related to inflammation and lipid synthesis in the liver is shown. D, Oil red O assay demonstrated that BA treatment significantly reduced lipid accumulation in AML12 hepatocytes that were treated with a fatty liver-related factor (palmitate 250 μM). E, Western blotting analysis was performed to detect phosphorylation levels of AMPK in nontreated and BA-treated AML12 mouse hepatocyte cells. n = 3–5 per group; means ± S.D.; $^{*}p < 0.05$, $^{**}p < 0.01$, $^{***}p < 0.001$. (For interpretation of the references to colour in this figure legend, the reader is referred to the Web version of this article.)

treated mice (Fig. 5A); compared with nontreated mice, BA-treated mice exhibited reduced liver weight (Fig. 5B). In support of this phenotype, real-time quantitative PCR data showed that inflammatory genes, including the macrophage marker F4/80, interleukin (IL)-1α, IL-1β, IL-6, tumor necrosis factor (TNF)-α, and lipogenic genes including sterol regulatory element-binding protein (SREBP)-1c, apolipoprotein C2 (ApoC2), retinol binding protein (RBP) 4, FAS, and stearoyl-coenzyme A desaturase (SCD) 1 were decreased in BA-treated mice (Fig. 5C), indicating that BA protected against HFD-induced liver damage. We also found that BA treatment prevented palmitate-induced hepatic steatosis in AML12 hepatocytes. According to oil red O staining, BA treatment significantly reduced lipid accumulation in AML12 hepatocytes treated with a fatty liver-related factor (palmitate 250 μM) (Fig. 5D). To understand the mechanism by which BA decreases fat accumulation in the liver at the molecular level, Western blotting analysis was performed, and as shown in Fig. 5E, BA increased the level of phosphorylated AMPK in the AML12 mouse liver cell line.

Discussion

In this study, we used a mouse model of HFD-induced obesity and observed decreased weight gain in BA-treated mice. BAT and WAT, including inguinal, perigonadal and mesenteric fat, were reduced, and lipid droplets were also reduced (Fig. 1A, C–F). Abdominal obesity is associated with an increased risk of cardiovascular diseases and insulin resistance [43], and our findings also provide evidence that BA protects against hepatic steatosis development (Fig. 5A). The effects of BA might be mediated through food intake, as decreased food intake would be expected to significantly affect body weight, which influences hepatic steatosis. In this study, however, there was no difference in food intake-induced increases in body weight between BA-treated and nontreated groups (Fig. 1B), suggesting that BA directly protects against obesity and hepatic steatosis independently of food intake. To investigate the antiadipogenic mechanism, the effect of BA on expression levels of genes associated with regulation of energy expenditure and fatty acid oxidation were

examined. In 3T3-L1 adipocytes, BA elevated levels of lipid oxidative gene expression compared with nontreated cells (Fig. 2B); mRNA levels of GPAT, DAT1, DGAT2, and FAS, which encode key enzymes in triacylglycerol synthesis, were also significantly decreased (Fig. 2C–F), as was expression of transcription factors required for adipocyte differentiation (PPARγ) (Fig. 2G). Accordingly, the visceral adiposity-suppressing effects of BA may be linked to increase in the expression of mitochondrial biogenesis-related genes and fatty acid oxidation. AMPK is a key regulator of proteins involved in lipogenesis and fatty acid oxidation in metabolic tissues [44]; thus, we investigated whether BA activates AMPK by assessing its phosphorylation. BA treatment drastically increased AMPK phosphorylation (Figs. 2H, 3E and 4D, 4E and 5E), indicating that BA inhibits adipocyte differentiation via activation of this regulator. BA may activate AMPK and selectively regulate expression of energy metabolism-related genes, eventually leading to both suppression of lipogenesis and degradation of fat.

The hallmark of dyslipidemia in obesity is hypertriglyceridemia in combination with the preponderance of high cholesterol and triglyceride [45]. Hyperinsulinemia, a biomarker of insulin resistance, is frequently accompanied by obesity [46], and the concentration of serum leptin is reported to be associated with general adiposity and reflects the body fat content [47]. This study shows that in HFD-fed mice, BA administration significantly reduced serum levels of cholesterol and triglyceride (Fig. 1G, H); insulin and leptin levels were also increased in the HFD group but significantly decreased by BA administration (Fig. 1I, J). Moreover, the weight of adipose tissues strongly correlated with the plasma leptin level. These results confirm that BA treatment had an antiobesity effect in the diet-induced obesity C57BL/6 mouse model.

In addition to inhibiting fat accumulation in WAT, the body fat-lowering effect of BA may also be due to enhanced thermogenesis capacity. Adaptive thermogenesis is defined as heat production in response to environmental temperature to protect the organism from exposure to cold [48]. Activation of UCP, a mitochondrial proton transporter, promotes uncoupled respiration and thereby results in dissipation of oxidation energy as heat, and HFD-induced downregulation of PGC-1α decreases expression of UCP and eventually suppresses uncoupled respiration. In the present study, BA simultaneously reversed the HFD-induced downregulation of PGC-1α and UCP expression in the BAT and muscle tissue of mice (Figs. 3B and 4C). Therefore, we suggest that the visceral fat-pad weight-lowering effects of BA may be associated with increased expression of genes involved in uncoupled respiration in the visceral adipose tissue of HFD-fed mice.

Accumulating evidence indicates that SREBP-1c is a critical regulator of hepatic lipid metabolism. This transcription factor stimulates expression of several enzymes involved in liver fatty acid synthesis and glucose transport, gluconeogenesis, and lipolysis [49], and recent studies of obese patients have reported that increased SREBP-1c expression is strongly associated with fatty liver disease [50]. As shown in Fig. 5C, SREBP-1c gene expression was repressed in HFD-fed mice treated with BA. The liver steatosis attenuation observed in these mice was related to this effect and may also be linked to the other signals of liver protection elicited by BA, including reduced expression of proinflammatory cytokines and lipogenic genes, inhibiting fatty mass accumulation and body weight. We determined that BA drastically increased AMPK phosphorylation in the AML12 cell line, thus indicating that BA inhibits adipocyte differentiation via activation of AMPK. These results suggest that BA activates AMPK and that BA inactivates SREBP-1c transcription and inhibits hepatic steatosis in HFD-induced animal models. We determined the toxicity of BA treatment in each cell line and found no toxicity within the indicated dose range (Supplementary Fig. 1B-E). Many stressors induce AMPK activation, and we confirmed that AMPK activation is a result of BA-induced cell injury. Our findings suggest that BA plays a role in AMPK activation, which regulates energy metabolism.

Conflicts of interest

The authors declare that they have no competing interests.

Author contributions

K.-D.K., H.-Y.J. and J.-B.K. designed the research; K.-D.K., B.K., H.G.R., H.-Y.J., J.J. and I.K. performed the research; H.-Y.J., H.Y.Y. and K.-D.K. wrote the paper; and C.-K.H., B.-H.C., C.H.P., K.-T.K., S.F., S.H.Y. and J.-B.K. critically evaluated the paper.

Acknowledgments

This study was supported by the Technological Innovation R&D Program (SA114125) funded by the Small and Medium Business Administration (SMBA, Republic of Korea). This research was also supported by a grant from the Korea Health Technology R&D Project through the Korea Health Industry Development Institute (KHIDI), funded by the Ministry of Health & Welfare, Republic of Korea (Grant Number: HI16C1501).

Appendix A. Supplementary data

Supplementary data to this article can be found online at https://doi.org/10.1016/j.numecd.2018.12.001.

References

[1] Reaven GM. Role of insulin resistance in human disease. Diabetes 1988;37:1595–607. https://doi.org/10.2337/diab.37.12.1595.
[2] Grundy SM. Drug therapy of the metabolic syndrome: minimizing the emerging crisis in polypharmacy. Nat Rev Drug Discov 2006;5:295–309. https://doi.org/10.1038/nrd2005.
[3] Despres J-P, Lemieux I. Abdominal obesity and metabolic syndrome. Nature 2006;444:881–7.
[4] Boudina S, Sena S, O'Neill BT, Tathireddy P, Young ME, Abel ED. Reduced mitochondrial oxidative capacity and increased mitochondrial uncoupling impair myocardial energetics in obesity. Circulation

2005;112:2686–95. https://doi.org/10.1161/circulationaha.105.554360.
[5] Kim J-Y, Hickner RC, Cortright RL, Dohm GL, Houmard JA. Lipid oxidation is reduced in obese human skeletal muscle. Am J Physiol Endocrinol Metabol 2000;279:E1039–44. https://doi.org/10.1152/ajpendo.2000.279.5.E1039.
[6] Dulloo AG, Seydoux J, Jacquet J. Adaptive thermogenesis and uncoupling proteins: a reappraisal of their roles in fat metabolism and energy balance. Physiol Behav 2004;83:587–602. https://doi.org/10.1016/j.physbeh.2004.07.028.
[7] Cannon B, Nedergaard J. Brown adipose tissue: function and physiological significance. Physiol Rev 2004;84:277–359. https://doi.org/10.1152/physrev.00015.2003.
[8] Rothwell NJ, Stock MJ. A role for brown adipose tissue in diet-induced thermogenesis. Nature 1979;281:31–5. https://doi.org/10.1038/281031a0.
[9] Himms-Hagen J. Brown adipose tissue thermogenesis: interdisciplinary studies. Faseb J 1990;4:2890–8. https://doi.org/10.1096/fasebj.4.11.2199286.
[10] Bachman ES, Dhillon H, Zhang C-Y, Cinti S, Bianco AC, Kobilka BK, et al. βAR signaling required for diet-induced thermogenesis and obesity resistance. Science 2002;297:843–5. https://doi.org/10.1126/science.1073160.
[11] Hamann A, Flier JS, Lowell BB. Decreased brown fat markedly enhances susceptibility to diet-induced obesity, diabetes, and hyperlipidemia. Endocrinology 1996;137:21–9. https://doi.org/10.1210/endo.137.1.8536614.
[12] Feldmann HM, Golozoubova V, Cannon B, Nedergaard J. UCP1 ablation induces obesity and abolishes diet-induced thermogenesis in mice exempt from thermal stress by living at thermoneutrality. Cell Metabol 2009;9:203–9. https://doi.org/10.1016/j.cmet.2008.12.014.
[13] Lowell BB, S-Susulic V, Hamann A, Lawitts JA, Himms-Hagen J, Boyer BB, et al. Development of obesity in transgenic mice after genetic ablation of brown adipose tissue. Nature 1993;366:740–2. https://doi.org/10.1038/366740a0.
[14] Kontani Y, Wang Y, Kimura K, Inokuma KI, Saito M, Suzuki-Miura T, et al. UCP1 deficiency increases susceptibility to diet-induced obesity with age. Aging Cell 2005;4:147–55. https://doi.org/10.1111/j.1474-9726.2005.00157.x.
[15] Kopecky J, Clarke G, Enerback S, Spiegelman B, Kozak LP. Expression of the mitochondrial uncoupling protein gene from the aP2 gene promoter prevents genetic obesity. J Clin Invest 1995;96:2914–23. https://doi.org/10.1172/JCI118363.
[16] Watanabe M, Houten SM, Mataki C, Christoffolete MA, Kim BW, Sato H, et al. Bile acids induce energy expenditure by promoting intracellular thyroid hormone activation. Nature 2006;439:484–9. https://doi.org/10.1038/nature04330.
[17] Kharitonenkov A, Shiyanova TL, Koester A, Ford AM, Micanovic R, Galbreath EJ, et al. FGF-21 as a novel metabolic regulator. J Clin Invest 2005;115:1627–35. https://doi.org/10.1172/JCI23606.
[18] Xu J, Lloyd DJ, Hale C, Stanislaus S, Chen M, Sivits G, et al. Fibroblast growth factor 21 reverses hepatic steatosis, increases energy expenditure, and improves insulin sensitivity in diet-induced obese mice. Diabetes 2009;58:250–9. https://doi.org/10.2337/db08-0392.
[19] Kim H, Choung S-Y. Anti-obesity effects of *boussingaulti gracilis* Miers var. *pseudobaselloides* Bailey via activation of AMP-activated protein kinase in 3T3-L1 cells. J Med Food 2012;15:811–7. https://doi.org/10.1089/jmf.2011.2126.
[20] Baar K, Wende AR, Jones TE, Marison M, Nolte LA, Chen M, et al. Adaptations of skeletal muscle to exercise: rapid increase in the transcriptional coactivator PGC-1. Faseb J 2002;16:1879–86. https://doi.org/10.1096/fj.02-0367com.
[21] Puigserver P, Wu Z, Park CW, Graves R, Wright M, Spiegelman BM. A cold-inducible coactivator of nuclear receptors linked to adaptive thermogenesis. Cell 1998;92:829–39. https://doi.org/10.1016/S0092-8674(00)81410-5.
[22] Puigserver P, Spiegelman BM. Peroxisome proliferator-activated receptor-γ coactivator 1α (PGC-1α): transcriptional coactivator and metabolic regulator. Endocr Rev 2003;24:78–90. https://doi.org/10.1210/er.2002-0012.
[23] Liang H, Balas B, Tantiwong P, Dube J, Goodpaster BH, O'Doherty RM, et al. Whole body overexpression of PGC-1α has opposite effects on hepatic and muscle insulin sensitivity. Am J Physiol Endocrinol Metabol 2009;296:E945–54. https://doi.org/10.1152/ajpendo.90292.2008.
[24] Wareski P, Vaarmann A, Choubey V, Safiulina D, Liiv J, Kuum M, et al. PGC-1α and PGC-1β regulate mitochondrial density in neurons. J Biol Chem 2009;284:21379–85. https://doi.org/10.1074/jbc.M109.018911.
[25] Alakurtti S, Mäkelä T, Koskimies S, Yli-Kauhaluoma J. Pharmacological properties of the ubiquitous natural product betulin. Eur J Pharm Sci 2006;29:1–13. https://doi.org/10.1016/j.ejps.2006.04.006.
[26] Yogeeswari P, Sriram D. Betulinic acid and its derivatives: a review on their biological properties. Curr Med Chem 2005;12:657–66. https://doi.org/10.2174/0929867053202214.
[27] Cichewicz RH, Kouzi SA. Chemistry, biological activity, and chemotherapeutic potential of betulinic acid for the prevention and treatment of cancer and HIV infection. Med Res Rev 2004;24:90–114. https://doi.org/10.1002/med.10053.
[28] Szejtli J. Introduction and general overview of cyclodextrin chemistry. Chem Rev 1998;98:1743–54. https://doi.org/10.1021/cr970022c.
[29] Fulda S, Scaffidi C, Susin SA, Krammer PH, Kroemer G, Peter ME, et al. Activation of mitochondria and release of mitochondrial apoptogenic factors by betulinic acid. J Biol Chem 1998;273:33942–8. https://doi.org/10.1074/jbc.273.51.33942.
[30] Costantini P, Jacotot E, Decaudin D, Kroemer G. Mitochondrion as a novel target of anticancer chemotherapy. J Natl Cancer Inst 2000;92:1042–53. https://doi.org/10.1093/jnci/92.13.1042.
[31] Fulda S, Debatin KM. Betulinic acid induces apoptosis through a direct effect on mitochondria in neuroectodermal tumors. Med Pediatr Oncol 2000;35:616–8. https://doi.org/10.1002/1096-911X(20001201)35:6<616::AID-MPO27>3.0.CO;2-N.
[32] Schühly W, Heilmann J, Çalis I, Sticher O. New triterpenoids with antibacterial activity from *Zizyphus joazeiro*. Planta Med 1999;65:740–3. https://doi.org/10.1055/s-1999-14054.
[33] Steele JC, Warhurst DC, Kirby GC, Simmonds MS. *In vitro* and *in vivo* evaluation of betulinic acid as an antimalarial. Phytother Res 1999;13:115–9. https://doi.org/10.1002/(SICI)1099-1573(199903)13:2<115::AID-PTR404>3.0.CO;2-1.
[34] Kwon HJ, Shim JS, Kim JH, Cho HY, Yum YN, Kim SH, et al. Betulinic acid inhibits growth factor-induced *in vitro* angiogenesis via the modulation of mitochondrial function in endothelial cells. Jpn J Cancer Res 2002;93:417–25. https://doi.org/10.1111/j.1349-7006.2002.tb01273.x.
[35] Pavlova NI, Savinova OV, Nikolaeva SN, Boreko EI, Flekhter OB. Antiviral activity of betulin, betulinic and betulonic acids against some enveloped and non-enveloped viruses. Fitoterapia 2003;74:489–92. https://doi.org/10.1016/S0367-326X(03)00123-0.
[36] Tan Y, Yu R, Pezzuto JM. Betulinic acid-induced programmed cell death in human melanoma cells involves mitogen-activated protein kinase activation. Clin Cancer Res 2003;9:2866–75.
[37] Yun Y, Han S, Park E, Yim D, Lee S, Lee C-K, et al. Immunomodulatory activity of betulinic acid by producing pro-inflammatory cytokines and activation of macrophages. Arch Pharm Res 2003;26:1087. https://doi.org/10.1007/BF02994763.
[38] Singab ANB, El-Beshbishy HA, Yonekawa M, Nomura T, Fukai T. Hypoglycemic effect of Egyptian morus alba root bark extract: effect on diabetes and lipid peroxidation of streptozotocin-induced diabetic rats. J Ethnopharmacol 2005;100:333–8. https://doi.org/10.1016/j.jep.2005.03.013.
[39] de Melo CL, Queiroz MGR, Filho ACVA, Rodrigues AM, de Sousa DF, Almeida JGL, et al. Betulinic acid, a natural pentacyclic triterpenoid, prevents abdominal fat accumulation in mice fed a high-fat diet. J Agric Food Chem 2009;57:8776–81. https://doi.org/10.1021/jf900768w.
[40] Quan HY, Kim DY, Kim SJ, Jo HK, Kim GW, Chung SH. Betulinic acid alleviates non-alcoholic fatty liver by inhibiting SREBP1 activity via the AMPK–mTOR–SREBP signaling pathway. Biochem Pharmacol 2013;85:1330–40. https://doi.org/10.1016/j.bcp.2013.02.007.
[41] Jung H-Y, Kim Y-H, Kim I-B, Jeong JS, Lee J-H, Do M-S, et al. The Korean mistletoe (*Viscum album coloratum*) extract has an anti-obesity effect and protects against hepatic steatosis in mice with high-fat diet-induced obesity. Evid Based Complement Altern 2013;2013:9. https://doi.org/10.1155/2013/168207.

[42] Jung H-Y, Lee A-N, Song T-J, An H-S, Kim Y-H, Kim K-D, et al. Korean mistletoe (*Viscum album coloratum*) extract improves endurance capacity in mice by stimulating mitochondrial activity. J Med Food 2012;15:621–8. https://doi.org/10.1089/jmf.2010.1469.

[43] Wronska A, Kmiec Z. Structural and biochemical characteristics of various white adipose tissue depots. Acta Physiol (Oxf) 2012;205:194–208. https://doi.org/10.1111/j.1748-1716.2012.02409.x.

[44] Hardie DG. AMPK: a key regulator of energy balance in the single cell and the whole organism. Int J Obes 2008;32. S7–12, https://doi.org/10.1038/ijo.2008.116.

[45] Staiger H, Häring HU. Adipocytokines: fat-derived humoral mediators of metabolic homeostasis. Exp Clin Endocrinol Diabetes 2005;113:67–79. https://doi.org/10.1055/s-2004-830555.

[46] Lowell BB, Spiegelman BM. Towards a molecular understanding of adaptive thermogenesis. Nature 2000;404:652–60. https://doi.org/10.1038/35007527.

[47] Klop B, Elte J, Cabezas M. Dyslipidemia in obesity: mechanisms and potential targets. Nutrients 2013;5:1218. https://doi.org/10.3390/nu5041218.

[48] Tabák AG, Herder C, Rathmann W, Brunner EJ, Kivimäki M. Prediabetes: a high-risk state for diabetes development. Lancet 2012;379:2279–90. https://doi.org/10.1016/S0140-6736(12)60283-9.

[49] Yap F, Craddock L, Yang J. Mechanism of AMPK suppression of LXR-dependent Srebp-1c transcription. Int J Biol Sci 2011;7:645–50. https://doi.org/10.7150/ijbs.7.645.

[50] Pettinelli P, Videla LA. Up-regulation of PPAR-γ mRNA expression in the liver of obese patients: an additional reinforcing lipogenic mechanism to SREBP-1c induction. J Clin Endocrinol Metabol 2011;96:1424–30. https://doi.org/10.1210/jc.2010-2129.